The tardigrade *Hypsibius dujardini*, a new model for studying the evolution of development

Willow N. Gabriel[a],
Robert McNuff[b],
Sapna K. Patel[a],
T. Ryan Gregory[c],
William R. Jeck[a],
Corbin D. Jones[a],
Bob Goldstein[a,]

[a] Biology Department, University of North Carolina at Chapel Hill, Chapel Hill, NC 27599, USA
[b] Sciento, 61 Bury Old Road, Whitefield, Manchester, M45 6TB, England, UK
[c] Department of Integrative Biology, University of Guelph, Guelph, Ontario, Canada N1G 2W1

Abstract

Studying development in diverse taxa can address a central issue in evolutionary biology: how morphological diversity arises through the evolution of developmental mechanisms. Two of the best-studied developmental model organisms, the arthropod *Drosophila* and the nematode *Caenorhabditis elegans*, have been found to belong to a single protostome superclade, the Ecdysozoa. This finding suggests that a closely related ecdysozoan phylum could serve as a valuable model for studying how developmental mechanisms evolve in ways that can produce diverse body plans. Tardigrades, also called water bears, make up a phylum of microscopic ecdysozoan animals. Tardigrades share many characteristics with *C. elegans* and *Drosophila*that could make them useful laboratory models, but long-term culturing of tardigrades historically has been a challenge, and there have been few studies of tardigrade development. Here, we show that the tardigrade*Hypsibius dujardini* can be cultured continuously for decades and can be cryopreserved. We report that *H. dujardini* has a compact genome, a little smaller than that of *C. elegans* or *Drosophila*, and that sequence evolution has occurred at a typical rate. *H. dujardini* has a short generation time, 13–14 days at room temperature. We have found that the embryos of *H. dujardini* have a stereotyped cleavage pattern with asymmetric cell divisions, nuclear migrations, and cell migrations occurring in reproducible patterns. We present a cell lineage of the early embryo and an embryonic staging series. We expect that these data can serve as a platform for using *H. dujardini* as a model for studying the evolution of developmental mechanisms.

Keywords

Development;
Evolution;
Ecdysozoa;
Tardigrade;
Lineage;
Model system

Introduction

Recent advances in molecular phylogenies suggest that two well-studied model organisms, *Caenorhabditis elegans* (a nematode) and *Drosophila melanogaster* (an arthropod), are more closely related to each other than previously expected (Aguinaldo et al., 1997, Giribet and Ribera, 1998, Peterson and Eernisse, 2001,Copley et al., 2004 and Dopazo and Dopazo, 2005). Both phyla are members of the Ecdysozoa, one of the two protostome superclades. Other ecdysozoan phyla could be valuable models to study the evolution of development, since such phyla may maximize the chance to make use of both the vast biological information and the techniques that have been developed in *C.*

elegans and *Drosophila*. The other ecdysozoans comprise several of the least-studied animal phyla– loriciferans, kinorhynchs, priapulids, nematomorphs, onychophorans, and tardigrades (Fig. 1).

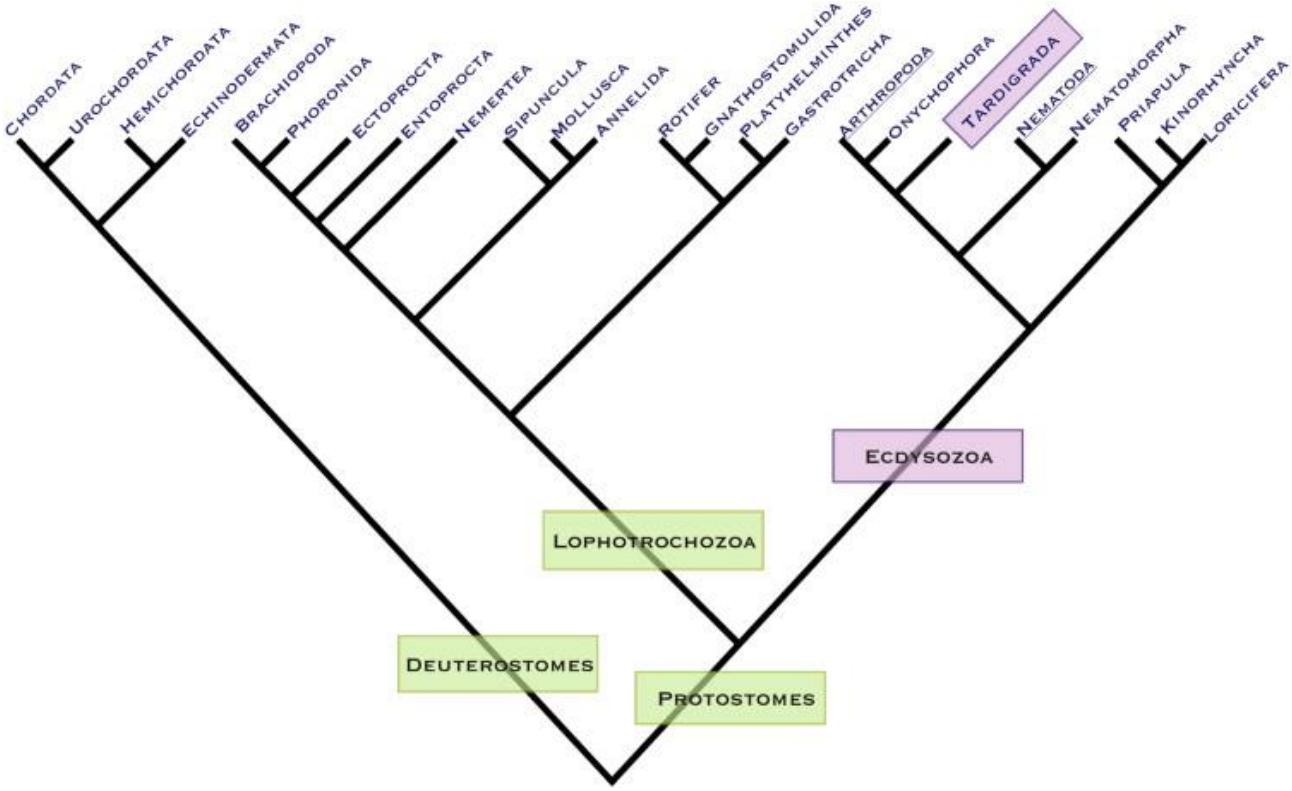

Fig. 1. Evolutionary position of the tardigrades (Aguinaldo et al., 1997, Giribet and Ribera, 1998, Garey et al., 1999,Garey, 2001, Peterson and Eernisse, 2001, Copley et al., 2004 and Dopazo and Dopazo, 2005). Protostome and deuterostome phyla are shown. Reprinted from Gabriel and Goldstein (2007).

Figure options

The current problem with using the non-model ecdysozoan phyla for such studies is that very little is known about development in any of these groups. There have been some studies of embryonic development (Hyman, 1951, Anderson, 1973 and Hejnol and Schnabel, 2005) and a few studies of developmental gene expression in these organisms (Panganiban et al., 1997, De Rosa et al., 1999, Grenier and Carroll, 2000 and Eriksson et al., 2005), but we lack basic developmental data such as reliable fate maps or cell lineages for ecdysozoans with stereotyped development outside of the nematodes (Goldstein, 2001) and arthropods (Hertzler and Clark, 1992 and Gerberding et al., 2002).

Tardigrades, also known as water bears, are a phylum of microscopic animals (Kinchin, 1994). The adults are typically up to half of a millimeter long and transparent, comprising a head plus four body segments, each with a ganglion, musculature, and a pair of limbs. They are famous for cryptobiosis: a dehydrated tardigrade can survive for years in a form known as a tun, which resists extreme temperatures and pressures. Tardigrades are aquatic and marine organisms and are often found in water films on mosses (Ramazzotti and Maucci, 1983). Fossil tardigrades from the Cambrian suggest that this is an ancient phylum (Müller et al., 1995). Nearly a thousand species of tardigrades have been described to date (Guidetti and Bertolani, 2005), and it is likely that several thousand more have yet to be discovered and described (Guil and Cabrero-Sañudo, 2007).

Tardigrades share many features with *C. elegans* and *Drosophila* that make them suitable lab models. They were, in fact, nearly chosen by Sydney Brenner instead of *C. elegans*, when Brenner was in search of a new model organism in the 1960's. Brenner chose instead the then little-studied *C. elegans* primarily because it has fewer neurons (S. Brenner, personal communication; Brenner, 2001). Tardigrades are reported to have a small and constant cell number, and they have a simple body plan (Kinchin, 1994).

There have been only a few studies of tardigrade development. Most of the research on tardigrades concerns instead their systematics, ecology, physiology, and descriptions of new species (Kinchin, 1994). Three important papers on tardigrade embryonic development were published before 1930 (Von Erlanger, 1895,Von Wenck,

1914 and Marcus, 1929). These papers described normal development, based almost exclusively on fixed embryos. Early cleavages were reported to be nearly equal, and epithelia were reported to form early, beginning as early as the 5th to 6th round of cell division. Films of embryos produced bySchmidt (1971) contradict some of the claims that were made by these early authors. More recently, transmission electron micrographs and descriptions of some developmental stages have been published (Eibye-Jacobsen, 1997). Cell lineage and ablation studies have been reported for the tardigrade *Thulinius stephaniae* by Hejnol and Schnabel (2005), who did not detect a stereotyped cleavage pattern that would allow cells to be reproducibly identified in early embryos.

To lay the groundwork for future studies of tardigrade development, we have developed long-term culture and cryopreservation techniques for a tardigrade species, *Hypsibius dujardini*. *H. dujardini* adults are optically clear, with much of their anatomy visible by light microscopy (Fig. 2) *H. dujardini* was kept in culture for six years by Ammermann (Ammermann, 1967). We show here that they can be cultured continously for decades and cryopreserved, and that their genome size, rate of sequence evolution, generation time, and pattern of early development can make them suitable model organisms for studying how development evolves. We report a cell lineage of the early embryo that features a stereotyped pattern of nuclear migrations, asymmetric cell divisions, and cell migrations, and an equivalence group. To further develop an infrastructure for future work on this organism, we describe development in an embryonic staging series.

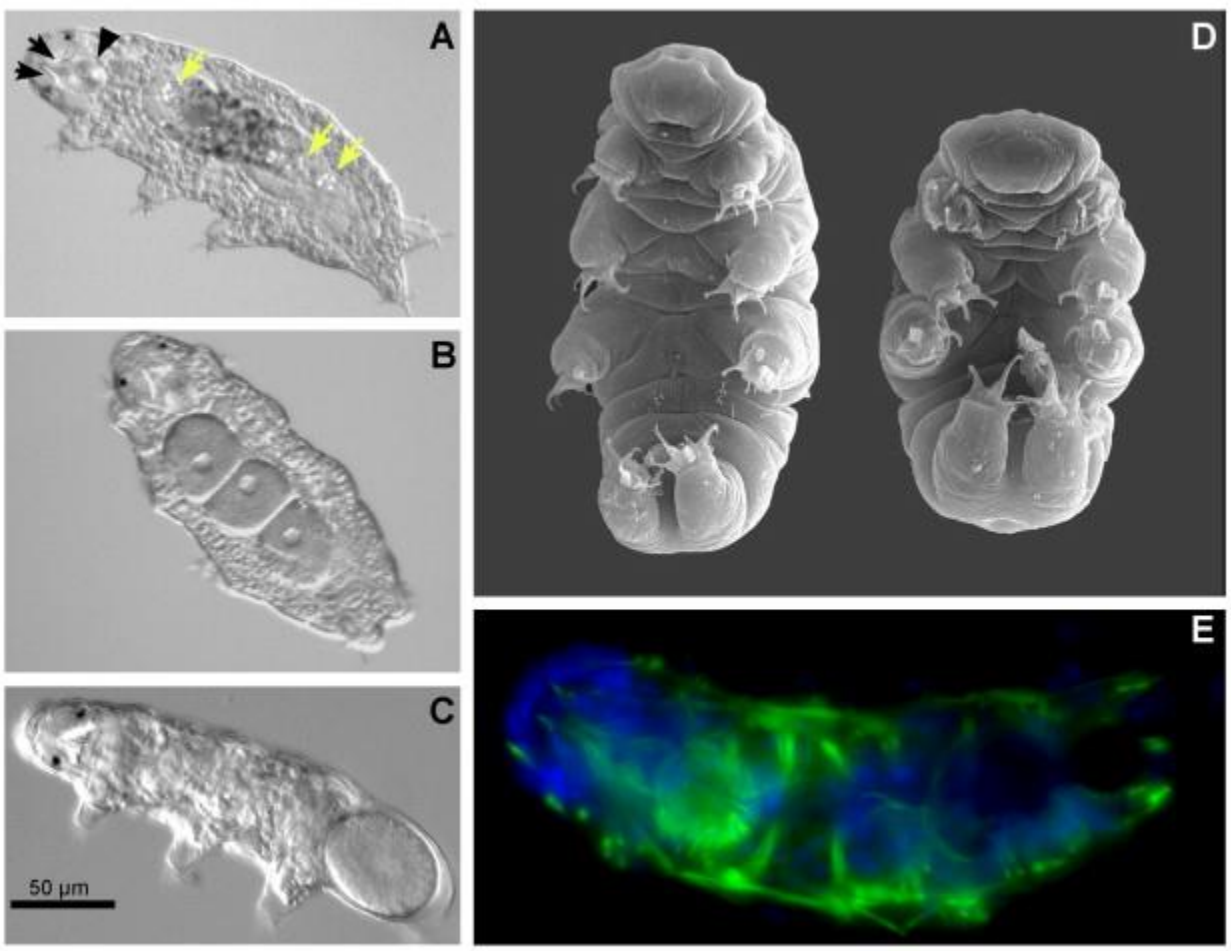

Fig. 2. Adult morphology of *H. dujardini.* (A) The morphologically distinct midgut is discernible by the presence of algae (dark matter in center of tardigrade) in the lumen and by birefringent granules (some marked by yellow arrows). Black arrowhead indicates the muscular pharynx. Black arrows point to stylets. Eyespots are visible as black dots lateral to the stylets. (B) After feeding, embryos are produced parthenogenetically. Three oocytes are visible in the center of this tardigrade. (C) Tardigrade laying an embryo as it molts. The tardigrade will exit its cuticle through the mouth opening, leaving embryos to develop in the cast off exuvia. (D) Two individual adults imaged by scanning electron microscopy, ventral views. Adults are ~ 500 μ m long. (E) Phalloidin and DAPI-stained animal showing muscle and pharynx (green) and nuclei (blue).

Figure options

Materials and methods

Culture methods

H. dujardini was collected by R.M. on 13 November 1987 from a benthic sample of a pond in Darcy Lever, Bolton, Lancashire, England (British National Grid Reference SD741078). Monoxenic cultures were maintained in 250 ml Erlenmeyer flasks containing 150 ml of Chalkley's Medium (5 ml of each of the following stock solutions per liter in dH_20: NaCl, 2 g/100 ml dH_20; KCl, 0.08 g/100 ml dH_20; $CaCl_2$, 0.12 g/100 ml dH_20) enriched with 2% soil extract (soil extract is the supernatant of 1 part fertile, humus-enriched soil to 2 parts tap water autoclaved and allowed to settle for a few days), and fed 3–5 ml per culture of concentrated cells from a *Chlorococcum* sp. culture. Subcultures were generated as cultures peaked, every 4–6 weeks. Cultures were maintained at 10–18 °C in a 14 h light/10 h dark cycle.

For collecting embryos in the laboratory, small cultures of tardigrades were kept in 60 mm glass Petri dishes in commercial bottled spring water (Crystal Geyser or Deer Park) at room temperature in a shaded location. These cultures were fed *Chlorococcum* sp. algae and water was changed once every ten days. Hundreds of tardigrades per Petri dish can be reared continuously in the lab at room temperature in this manner.

Microscopy and lineaging

For live imaging, *H. dujardini* embryos were mounted on uncoated glass microscope slides in bottled spring water with glass microspheres (diameter 49.21 ± 0.72 μm, range 47.0–51.4 μm, Whitehouse Scientific) used as spacers. 4-D differential interference contrast (DIC) microscopy was carried out on a C2400-07 Hamamatsu Newvicon (Hamamatsu Photonics) or a SPOT2 (Diagnostic Instruments) camera mounted on a Nikon Eclipse 800 microscope (Nikon Instrument Group). Images were acquired at 1 μm optical sections every 1–5 min during embryogenesis and analyzed with either 4D Viewer (LOCI, University of Wisconsin, Madison) or Metamorph v. 6.3r5 (Molecular Devices). Some images were false-colored using Adobe Photoshop 7.0. Embryos were filmed starting either from very early stages (meiosis-16 cell stage) through at least initiation of segmentation (~ 20 h of development) (*n* = 19 for the staging series and 4 for lineaging, seeMovie S1); or from the initiation of segmentation to hatching (*n* = 9, see Movie S2). Lineages were reconstructed by recording the time and orientation of each cell division in each recording. A program was written in BASIC to draw out the lineage with error bars using data pasted from an Excel spreadsheet. Scanning electron microscopy was performed as before (Gabriel and Goldstein, 2007).

DAPI staining

Embryos were removed from the parental exuvia by slicing with 25 gauge hypodermic needles and then fixed in absolute methanol for 20 min at 4 °C, followed by a 90%–70%–50% methanol series at room temperature (RT). Embryos were then post-fixed in 4% paraformaldehyde in 0.5× PBT (0.5× phosphate buffered saline with 0.05% Triton X-100) for 10 min at RT. Sonication was carried out in this fixative on a Branson 250 sonifier at an amplitude of 2.2 with a constant duty cycle for 4 pulses of 5 s each, with 15 s recovery on ice between each pulse. Embryos were then allowed to recover for 15 min on ice followed by 5 washes of 5 min each in 0.5× PBT. DAPI (5 μg/μl) was added to the next wash of 20 min, followed by two subsequent washes of 5 min each. Embryos were then mounted on slides that were coated in 0.2% gelatin, 0.02% chrome alum, 0.1% polylysine, and 1 mM azide.

Genome size calculation

The haploid nuclear genome size of *H. dujardini* was estimated by Feulgen image analysis densitometry (FIA) and flow cytometry (FCM). For FIA, specimens were air-dried whole on microscope slides and stained according to the protocol of Hardie et al. (2002). Briefly, slides were post-fixed overnight in 85% methanol, 10% formalin, 5% glacial acetic acid, rinsed in running tap water, and hydrolyzed for 2 h in 5 N HCl before a 2-h staining in fresh Schiff reagent and a series of tap water, bisulfite, and distilled water rinses. A total of 75 nuclei from three individuals were analyzed densitometrically using the Bioquant Life Science v8.00.20 image analysis program and compared against the integrated optical densities of hemocyte nuclei from *D. melanogaster* Oregon R strain (1C = 175 Mb) and *Tenebrio molitor* (1C = 510 Mb).

FCM estimates were performed on two samples of tardigrades following the protocol of De Salle et al. (2005)as follows. A sample of live tardigrades was centrifuged and the collected animals added to 2 ml Kontes dounce tissue grinders containing Galbraith buffer. A head from an individual of *D. melanogaster* was added to each tube and ground gently with the tardigrades to free nuclei before being filtered through 30 μm nylon mesh to remove debris. Propidium iodide (50 μl at 1 mg/ml) was added to both tubes and allowed to bind to the DNA for

approximately 2 h. The co-stained *H. dujardini* and *D. melanogaster* nuclei were analyzed using a BD FACSCalibur flow cytometer at 488 nm laser excitation. Roughly 5000 tardigrade nuclei were analyzed per sample.

Phylogenetic analysis

For all genes other than 18s rDNA, we queried the *H. dujardini* sequences in Genbank using BLAST to identify sequences corresponding to genes that are present in *D. melanogaster*, *C. elegans*, and *Homo sapiens*. For 18s, we used sequences available from Genbank and prior studies (Garey et al., 1999 and Nichols et al., 2006) for *H. dujardini*, *D. melanogaster*, *C. elegans*, *H. sapiens*, *Priapulus caudatus*,*Milnesium tardigradum*, *Macrobiotus hufelandi*, *T. stephaniae*, *Artemia salina*, *Gordius aquaticus*, and *Mus musculus*. We analyzed *14-3-3 zeta* (*14-3-3 zeta*), *cathD* (*cathD*), *sideroflexin* (*CG11739*), *glycogen synthase* (*CG6904*), *DEAH box polypeptide* (*CG8241*), *Cysteine proteinase-1* (*Cp1*), *Elongation factor 1-alpha-48D* (*Ef1-alpha-48D*), *Eukaryotic initiation factor 4a* (*eIF-4a*), *GDP dissociation inhibitor* (*Gdi*), *Minute*(*2) 21AB* (*M(2)21AB*), *Multidrug-Resistance like Protein 1* (*MRP*), *Phosphoglycerate kinase* (*Pgk*),*Proteasome 25 kDa subunit* (*Pros25*), *Proteasome alpha 7 subunit* (*Pros* α*7*), *Qm* (*Qm*), *Ribosomal protein L10Ab* (*RpL10Ab*), *Ribosomal protein L7A* (*RpL7A*), *Ribosomal protein S18* (*RpS18*), *Ribosomal protein S3A*(*RpS3A*), and *Ribosomal protein S6* (*RpS6*). With the exception of 18s, the evolutionary distances among these taxa made nucleotide alignments problematic. We therefore translated all coding sequence and performed protein alignments using ClustalW (Thompson et al., 1994). All alignments were visually inspected. These were analyzed using the Bayesian approach for phylogeny estimation implemented in MrBayes version 3.1.2 (Huelsenbeck and Ronquist, 2001), which uses a Markov Chain Monte Carlo algorithm (MCMC) for exploring the credibility of any particular phylogenetic tree. After specifying the appropriate model (see below), we analyzed each gene independently and all genes as a concatenated sequence.

Any phylogenetic reconstruction using protein sequences requires the specification of a protein substitution matrix or model. To determine the most appropriate model in this particular case, we analyzed the data using four different commonly used protein substitution models: Dayhoff, Poisson, Jones, and mixed model, which is a fixed rate model empirically estimated from the actual data using a MCMC sampler (Dayhoff et al., 1978,Bishop and Friday, 1987, Jones et al., 1992 and Huelsenbeck and Ronquist, 2001). For each protein substitution model and each sequence in our data set, we ran our MCMC for 50,000 generations (sampling the chain every 20 generations) after a burn-in of 10,000 generations. Of the 19 genes analyzed, five showed inconsistent topology among the models. For three of the five showing inconsistent topology, the credibility values were below 80 – the nominal threshold for Bayesian analyses – and thus considered unresolved by all models. As for branch length, the Poisson model showed a higher degree of inconsistency with the other three in branch length, though branch lengths were usually consistent. The concatenated tree produced topologically identical trees under all models and little variation in branch length. In general, the estimated mixed model performed best and was used for subsequent analyses.

For 18s, we used a Generalized Time Reversible model and gamma distributed rate variation. For each gene, we ran the MCMC for 1,000,000 generations after an initial burn in of 250,000 generations. We sampled the chain every 100 generations. Trees were summarized in MrBayes and then visualized using TreeView (Page, 1996). As noted above, 80% credibility score was considered support for a particular node.

Our null hypothesis of equal rates of amino acid evolution implies that the ratio of rates of amino acid change between two taxa should be around one. To test this null, we compared the number of genes with branch length ratios above and below one for each pair of taxa. A simple χ^2 test was then used to compare the counts from the two groups.

Results

Identification of a suitable tardigrade species

We attempted to identify a tardigrade species with optically clear embryos, so that we could follow cell divisions by optically sectioning live embryos using differential interference contrast (DIC) microscopy, and with small embryos and fast embryonic cell cycles, as this can suggest a small genome (Gregory, 2001). Several strains from biological supply companies and wild strains were examined. DIC recordings of embryos produced by one culture (see below) revealed that the embryos are clear, about 60 μm long, and early embryonic cell cycles are less than 1 h in length at room temperature. We sent a sample of this culture to Dr. Roberto Bertolani, who identified the tardigrade as *H. dujardini* (R. Bertolani, personal communication), a cosmopolitan, moss, and freshwater-dwelling species named after the French biologist Félix Dujardin (Doyère, 1840 and Kinchin, 1994). *H. dujardini* is a parthenogenetic species, with females laying eggs that undergo meiosis and then restore a diploid chromosome

number by reduplicating chromosomes, rather than by fertilization (Ammermann, 1967). Males have also been described, suggesting that some populations of this species may reproduce sexually (Ramazzotti and Maucci, 1983). *H. dujardini* forms cryptobiotic tuns that can survive dessication if initially dehydrated slowly at high relative humidity (Wright, 1989 and Wright, 2001).

H. dujardini can be maintained in culture, has a rapid life cycle, and can be cryopreserved

Long-term culture of tardigrades has historically been a challenge (Ramazzotti and Maucci, 1983, Bertolani et al., 1994, Kinchin, 1994 and Altiero and Rebecchi, 2001). One of us (R.M.) collected tardigrades from a pond in Bolton, Lancashire, England in 1987, and has maintained descendants of the original collection in culture continuously for the past two decades. Stocks are maintained in glass Erlenmeyer flasks and are fed a non-motile unicellular alga in the genus *Chlorococcum*. Smaller stocks of several hundred animals can be maintained similarly with ease in 60 mm glass Petri dishes (see Materials and methods). Each adult produces approximately 3 embryos per laying (mean = 3.4 ± 1.9 SD, range 1–10, *n* = 1411 embryos). Embryos are laid during molting, with the embryos deposited in the shed exoskeleton, called an exuvia, and the adult crawls out of the exuvia soon after producing embryos (Fig. 2). Embryos develop in the cast off exuvia until hatching occurs 4 to 4.5 days later. We found that the generation time is 13–14 days at room temperature (mean 13.6 ± 0.8 SD, *n* = 67), which is consistent with an earlier estimate of 10–14 days (Ammermann and Bosse, 1968).

A previous success with short-term freezing (Bertolani et al., 2004) suggested that a long-term freezing protocol might be possible. We tested a modification of an existing *C. elegans* freezing protocol (Stiernagle, 2006), adding glycerol to 15% to a mixed-stage Petri plate stock of tardigrades, and freezing aliquots slowly to −80 °C by freezing in a closed styrofoam box. We found that cultures could be re-established from such frozen aliquots upon thawing 51 days later or 365 days later, with roughly 50% of the individuals from mixed-stage cultures surviving in each case.

H. dujardini has a compact genome

H. dujardini has 5 pairs of chromosomes (Ammermann, 1967). To determine the size of the *H. dujardini*genome, we performed Feulgen image analysis densitometry (FIA) and propidium iodide flow cytometry (FCM). FIA and FCM estimates were in agreement, suggesting a haploid genome size of ~ 75 Mb for *H. dujardini*. Twenty other tardigrade species have been assessed for genome size to date, but none have exhibited a genome quite this compact (range: 80 Mb to 800 Mb) (Bertolani et al., 1994, Bertolani et al., 2004 and Gregory, 2007). The *H. dujardini* genome is among the smallest so far identified for animals, less than half the size of the *D. melanogaster* genome (Fig. 3) and three-quarters as large as that of *C. elegans*. The only metazoan genome sizes reported to exceed this level of compactness are found in some nematodes (as low as ~ 30 Mb), the placozoan *Trichoplax adhaerens* (40 Mb), gastrotrichs (≥ 50 Mb), sponges (≥ 60 Mb), some polychaete annelids (≥ 60 Mb), and the larvacean *Oikopleura dioica* (70 Mb) (Gregory, 2007).

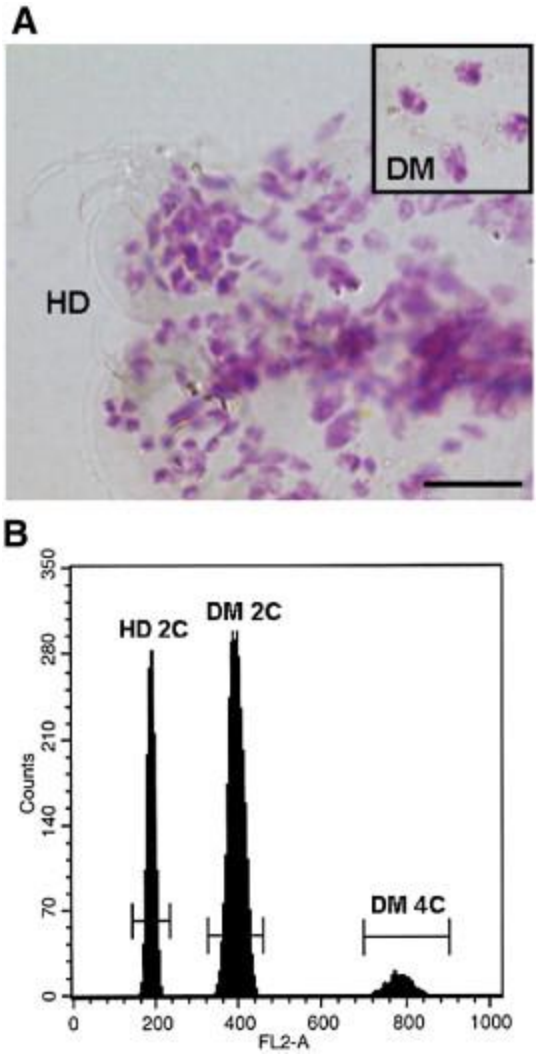

Fig. 3. *H. dujardini* has a compact genome. (A) Somatic nuclei of *H. dujardini* (HD), Feulgen-stained as an intact, air-dried specimen. Hemocyte nuclei from *D. melanogaster* (DM) at the same magnification are shown in the inset for comparison. (B) Flow cytometry results comparing propidium-iodide stained nuclei of *H. dujardini* (HD) and diploid (2C) and tetraploid (4C) nuclei of *D. melanogaster* (DM). The estimated genome size of *H. dujardini* is ~ 75 Mb.

Figure options

H. dujardini has had a typical rate of protein-coding sequence evolution

C. elegans protein-coding sequences have evolved at an unusually fast rate, whereas *Drosophila* sequences have evolved at a rate more typical for metazoans (Aguinaldo et al., 1997 and Mushegian et al., 1998). To determine relative rates of protein coding sequence evolution, we made use of the expressed sequence tags and genome survey sequences in Genbank contributed by M. Blaxter and colleagues, comparing patterns of amino acid evolution at 21 protein coding genes shared between *H. dujardini*, *D. melanogaster*, *C. elegans*, and *H. sapiens.* Given the evolutionary distances between these taxa, however, we first constructed a phylogenetic tree from both concatenated sequences of 21 protein coding genes and 18s rDNA to assist in our molecular evolutionary analysis (Fig. 4; Fig. S1). We then analyzed the rates of protein evolution for these 21 protein coding genes, using *H. sapiens* as an outgroup.

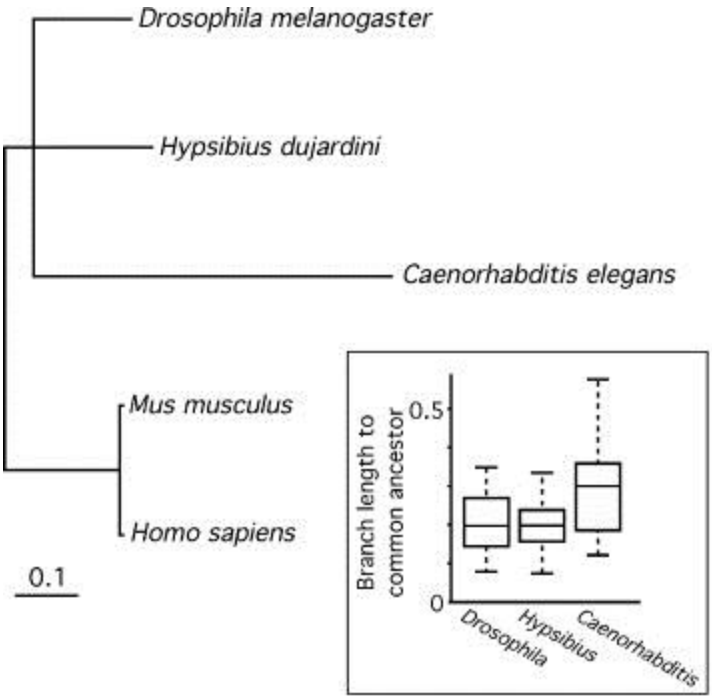

Fig. 4. *H. dujardini* has had a typical rate of sequence evolution. 18s rDNA phylogenetic tree is shown. Bayesian methods employing a Generalized Time Reversible model and gamma distributed rate variation were used for the reconstruction. Nodes below 80% credibility are considered unresolved and were collapsed. Inset: analysis of protein-coding sequences. Box-and-whiskers plot shows the smallest observation, lower quartile, median, upper quartile, and largest observations for branch lengths to the common ancestor of the three species, from 21 protein-coding genes analyzed.

Figure options

Our 18s data does not resolve the *C. elegans*, *D. melanogaster*, and *H. dujardini* polytomy (Fig. 4), nor does the concatenated sequence tree (Fig. S1). Among the 21 protein-coding genes we analyzed, this pattern was largely maintained with a slight bias towards grouping *C. elegans* and *H. dujardini* together (Fig. S1). This pattern generally held regardless of the model of protein evolution we used (see Materials and methods). Branch lengths – which reflect the rate of amino acid evolution – were also consistent across models, except for the few cases where the phylogeny could not be adequately resolved under a particular model. We then compared the ratio of the branch lengths of *H. dujardini* to *C. elegans* and *H. dujardini* to *D. melanogaster* for each gene (Fig. 4). If the rate of evolution is constant, we expect the mean ratios to be around one. We found that *H. dujardini* to *C. elegans* deviates in the direction of longer *C. elegans* branches significantly ($\chi^2 = 3.857$, $p = 0.0495$), and *H. dujardini* to *D. melanogaster* does not deviate ($\chi^2 = 0.048$, $p = 0.8273$). We conclude that the rate of protein evolution in *H. dujardini* is similar to that in *D. melanogaster* and, thus, like many other metzoan taxa.

H. dujardini has a stereotyped cleavage pattern

We generated multi-plane DIC recordings (Thomas et al., 1996) of *H. dujardini* embryos to examine embryonic development and to reconstruct a cell lineage through 7 rounds of cell division, to the ~ 128 cell stage. Cell lineages were traced in four individual embryos, and the resulting lineage and data on variability between individuals are presented (Fig. 5). Additional embryos were examined for several features that stood out among the four whose lineages were first traced–features including a stereotyped pattern of nuclear migrations that can predict the orientation of an embryonic axis, a stereotyped pattern of stem cell-like asymmetric divisions and division asynchrony, and an equivalence group of cells that ingress from the embryo surface to the interior.

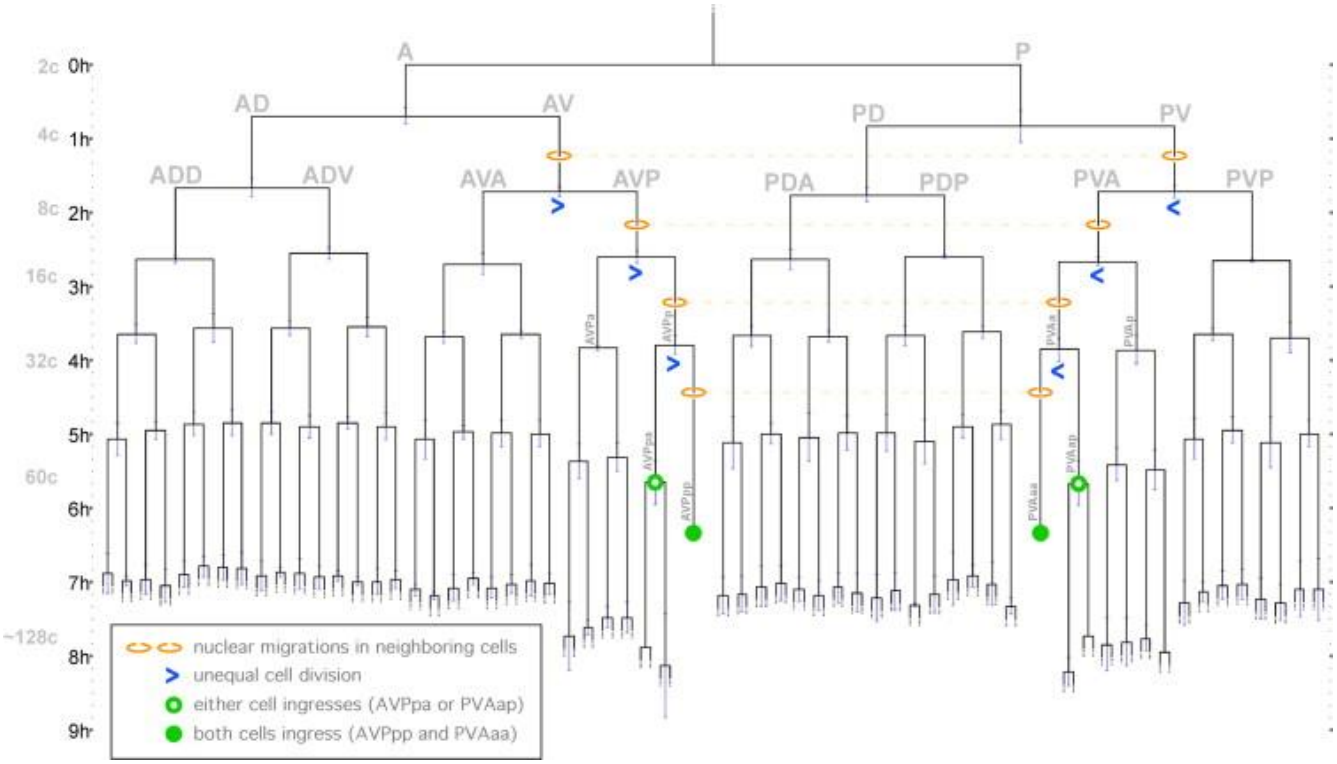

Fig. 5. Early embryonic cell lineage of *H. dujardini*. Timeline at left shows hours since first cleavage, with number of cells at each stage indicated in gray along timeline. Names of some cells are indicated in gray. Cell cycle lengths are means from up to four embryos, with 85% of the divisions drawn from 3 or 4 embryos. Blue error bars indicate variability between the embryos for each cell cycle length. The variability was calculated by the formula for standard deviation using data from 2–4 embryos, and no error bar is included where measurements were only available from a single embryo. Ingression to the center of the embryo is indicated (green circles) at the time of ingression. Cells that ingressed became migratory and were not followed further in the lineage. For AVPpa and PVAap, which ingress in some but not all embryos (two open green circles), division times are drawn for cases where that cell did not ingress.
Figure options

To our knowledge, based on our observations to date, the early embryonic cell lineage does not have obvious homologies among other phyla, in the sense that the lineages of diverse spiralian phyla do (Hyman, 1951 and Anderson, 1973). We therefore named cells based on their relationships to the embryonic axes, with capital letters A or P for the first two cells, and additional letters added to each cell's name based on the division orientations that produced the cell, an adaptation of the *C. elegans* cell naming system (Sulston et al., 1983). Small letters were used after the first three divisions. By this convention, the degree of relatedness between two cells can be deduced from the cells' names, and the number of letters in a cell's name indicates how many rounds of division occurred to produce that cell (Fig. 5).

The first embryonic cell division produced an anterior and a posterior blastomere, as in *C. elegans* and most other nematodes (Malakhov, 1994). In *H. dujardini*, this first division appeared to produce blastomeres of equal size. We were only able to assign anterior and posterior identity retrospectively, by examining embryos at elongation or examining where the pharynx, midgut, and hindgut formed later. The second division produced two dorsal and two ventral blastomeres of apparently equal size.

We found that the future ventral side can be predicted as early as the four cell stage by the position of a stereotyped pattern of nuclear migrations. Nuclei of the anterior and the posterior ventral cells (AV and PV) migrated toward each other, becoming nearly apposed to neighboring plasma membranes near the ventral-most part of the embryo. Mitotic spindles appeared by DIC microscopy to form where the nuclear envelopes disassembled, at an eccentric position in each ventral cell, and the resulting divisions were unequal, with two smaller cells (AVP and PVA) contacting each other on the ventral side of the embryo, and two larger cells (AVA and PVP) lateral to these (Fig. 5 and Fig. 6A). The smaller cells repeated this stem cell-like pattern of divisions for two more rounds, with unequal divisions producing smaller cells that underwent nuclear migrations toward each other near the ventral surface in each round. These divisions appeared similar to those that produce germline precursors in *C. elegans*, in that the smaller cell resulting from each unequal division continued to divide unequally (Deppe et

al., 1978). Because these unequal divisions produced daughters with distinct behaviors – one daughter dividing equally and the other undergoing a nuclear migration and dividing unequally – we refer to these as asymmetric cell divisions.

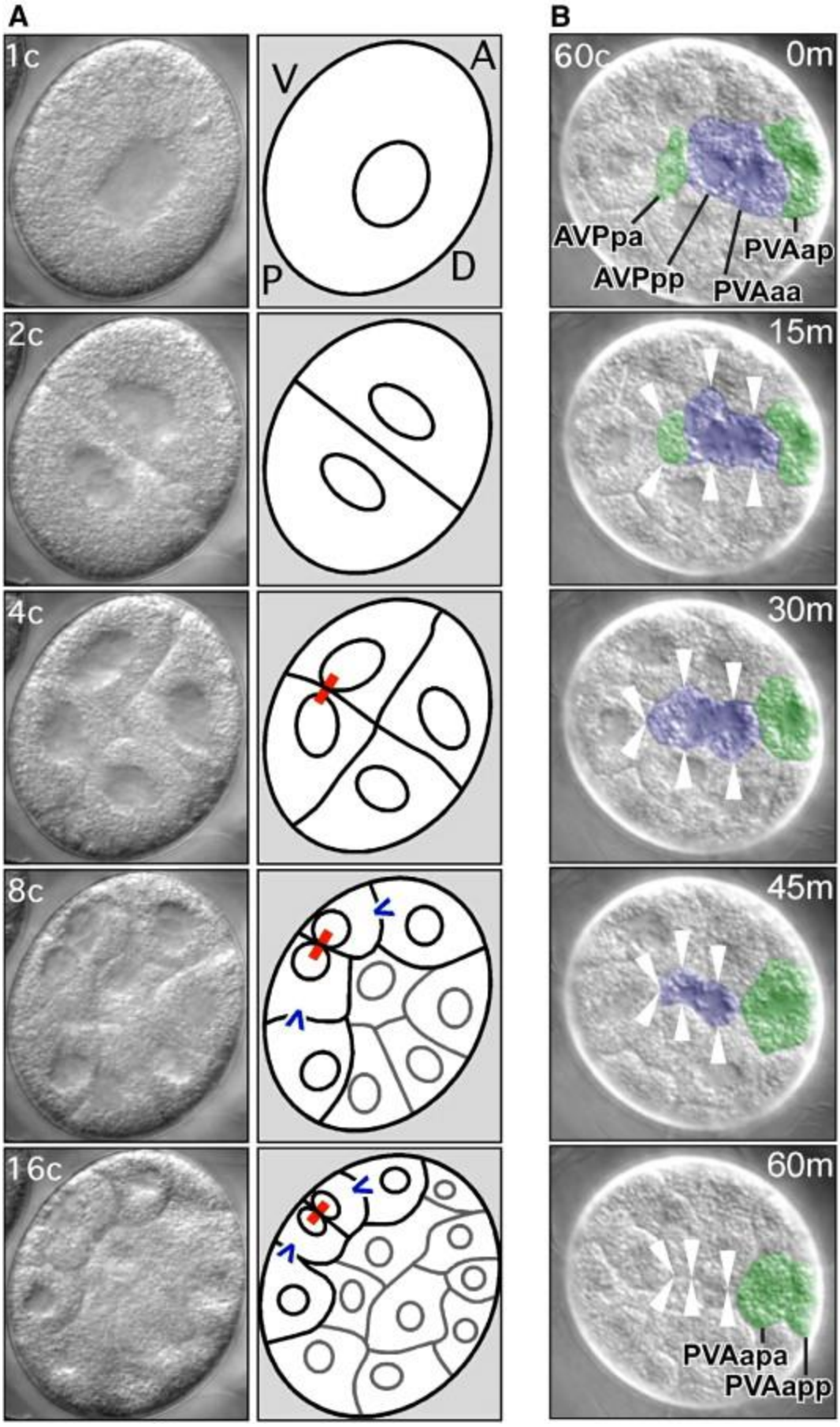
A
B
1c
2c
4c
8c
16c
V
A
P
D
60c
0m
15m
30m
45m
60m
AVPpa
AVPpp
PVAaa
PVAap
PVAapa
PVAapp

Fig. 6. Nuclear migrations, asymmetric cell divisions, cell ingression, and an equivalence group. (A) 1–16 cell stages by DIC microscopy (left) with drawings (right) indicating nuclear migrations near the ventral surface at the 4–16 cell stages (orange lines). Anterior, posterior, dorsal, and ventral are indicated in the 1 cell stage drawing (A, P, D, V, respectively). Cells resulting from asymmetric cell divisions are indicated at the 8 and 16 cell stages, with the direction of inequality in these divisions indicated (blue). (B) Ventral surface view of four cells, three of which invariably ingress at the 60 cell stage. Either AVPpa or PVAap (false-colored green) sinks from the ventral surface into the interior at this stage, followed by both of their sister cells AVPpp and PVAaa (blue). 15 min timepoints are shown. The edges of cells that neighbored the ingressing cells before they ingressed are indicated by arrowheads. The cell of this equivalence group that remains at the surface divides as the others complete ingression (see 60 min timepoint).
Figure options

Six cells of the eight cell stage embryo had lineages with synchronous or nearly synchronous divisions through the ~ 128 cell stage, whereas progeny of the two smallest cells of the eight cell stage (AVP and PVA) had distinctive cell cycle periods (Fig. 5). This was likely caused primarily by regulating the length of interphase rather than mitosis in specific cells, as the interval from cytokinesis to the following nuclear envelope breakdown varied between cells much more so than did the interval from nuclear envelope breakdown to the following cytokinesis (mean ± SD of 63.1 ± 21.7 min and 17.1 ± 2.7 min, respectively, among cells measured between the 5th and 6th round of division in an embryo).

The pattern of stem cell-like divisions resulted, at the 32 cell stage, in two small cells with nuclei apposed to neighboring plasma membranes near the ventral surface (AVPpp and PVAaa). These two cells invariably moved into the center of the embryo at the 60 cell stage (7/7 embryos). One other cell moved into the center of the embryo before this pair–the sister cell of either the anterior (3/7 embryos) or posterior (4/7 embryos) small cell, either AVPpa or PVAap (Fig. 5 and Fig. 6B). We conclude that either AVPpa or PVAap can adopt this behavior. Groups of cells whose fate assignments vary between individuals have been described before in a number of systems, and these are referred to as equivalence groups (Greenwald and Rubin, 1992). In such equivalence groups, cell fates are often determined by Notch-dependent signaling between cells, in which one cell adopting a specific fate inhibits others from taking the same fate (Simpson, 1997). Whether the AVPpa/PVAap equivalence group is resolved by intercellular signaling is not yet known. The fates of these early-ingressing cells are not yet known, although cells in the positions that these cells take have been called germ cell precursors by others (Marcus, 1929 and Hejnol and Schnabel, 2005).

An embryonic staging series

To provide a description of embryonic development and a standard basis for future studies on *H. dujardini*embryogenesis, we generated a staging series based on 4D videomicroscopy of 28 live tardigrade embryos (see Movies S1 and S2 for single plane views of examples) combined with DAPI staining of fixed embryos to reveal nuclei. Times below are given in hours post laying, and the time listed next to each stage heading is for the average time of onset for each stage. For embryos at the 1 to 16 cell stage (stages 1–5), timing of developmental events varied between embryos by no more 1.5 h; from 32 to 500 cells (stages 6–10), by no more than 3.6 h between embryos; and from stages 11 to 14 by no more than 6.7 h between embryos. For later stages, after muscle twitching starts, it is often more difficult to pinpoint the exact time of onset of developmental events, and a range of times is given for these stages.

Stage 1, one-cell (0–2 h post laying (hpl))

H. dujardini females produced broods of embryos approximately every 10 days under rearing conditions used. Females laid one-cell embryos, and the embryos completed meiosis after they had been laid. The mother generally exited the exuvia before her embryos completed meiosis. Embryos laid in a single cuticle had roughly synchronous developmental timing. Embryos appeared optically clear under differential interference contrast (DIC) microscopy. Embryos appeared isolecithal, with yolk granules uniformly distributed. During meiosis, individual chromosomes (2n = 10) could be visualized as clearings in the yolk granules by DIC microscopy (Fig. 7A; Fig. S2).

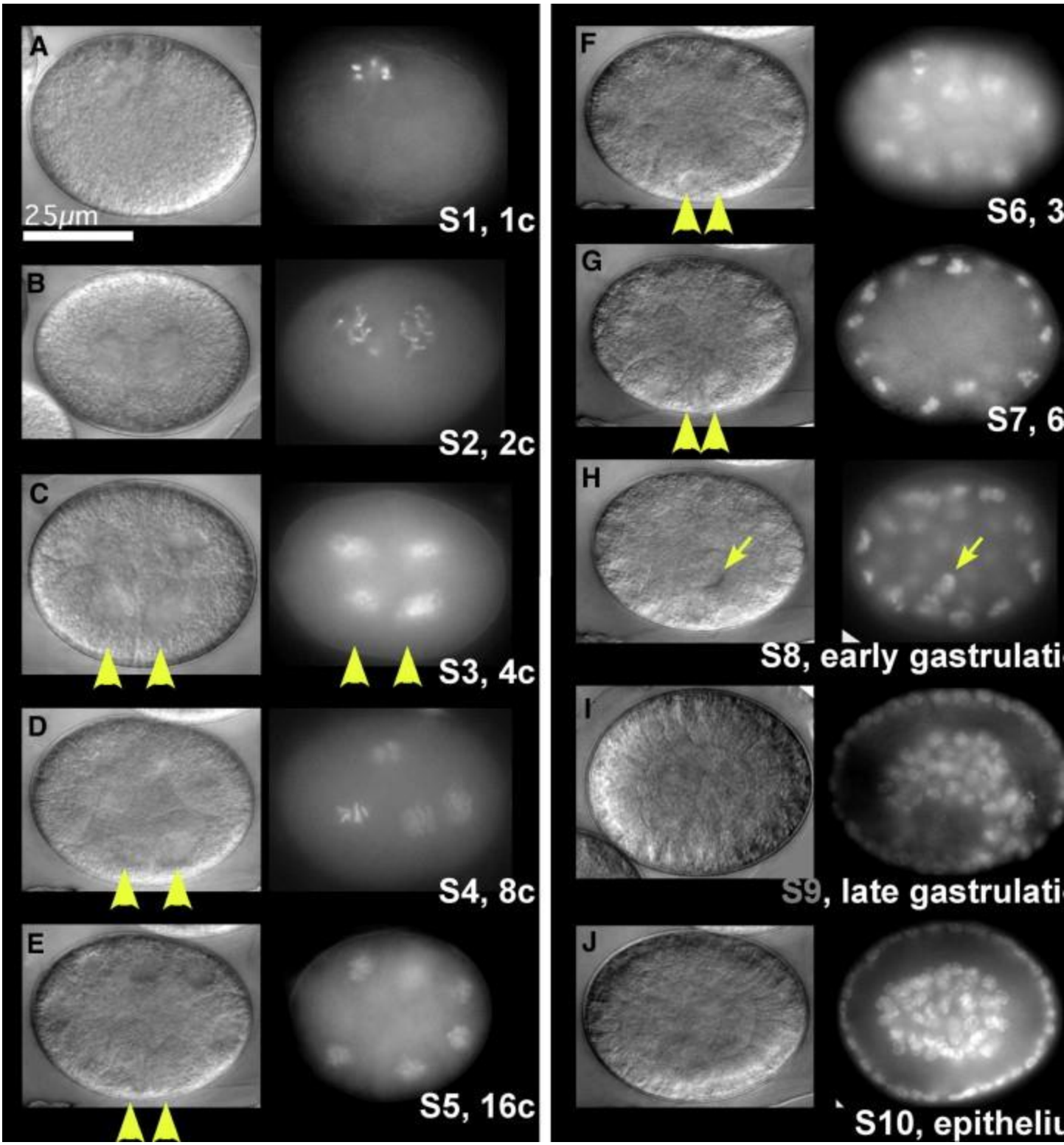

Fig. 7. Stages 1–10 of *H. dujardini* development. (A–J) *H. dujardini* embryos from meiosis through epithelium formation (0 to ~ 16.5 hpl). DIC images of live embryos are on the left, and fixed embryos at the same developmental stage that have been stained with DAPI are on the right. Yellow arrowheads indicate the two cells in the embryo with apposed nuclei. Yellow arrows in panel H point to the first cells to ingress. Embryos in panels C–J are oriented with ventral downwards.

Figure options

Stage 2, two-cell (2 hpl)

The first cleavage appeared total, and the plane of cytokinesis was generally perpendicular to the long axis of the embryo, dividing future anterior from posterior (Fig. 7B). The two daughter cells produced were visually indistinguishable. Yolk granules appeared to be evenly distributed during this and subsequent cell divisions. Nuclei were visible as clearings in the yolk granules under DIC microscopy.

Stage 3, four-cell (~ 3 hpl)

The second cleavage of each cell occurred roughly synchronously and was perpendicular to the first cleavage plane (Fig. 7C). After division, the nuclei of the ventral cells migrated as described in the cell lineage section above. These two cells occupied the future ventral side of the embryo.

Stages 4-6, 8 to 32 cells (~ 4-6.5 hpl)

Cell divisions continued to occur roughly synchronously, approximately once per hour, through the 32 cell stage. The cleavage pattern was radial, with most cleavage planes orthogonal to each previous division, producing a solid ball of cells, with no blastocoel evident at any stage (stages 4-6, Figs. 7D-F). At the 32 cell stage (stage 6, Fig. 7F), all 32 nuclei migrated apically. In the ventral cells, nuclear migrations and asymmetric divisions occurred as described in the cell lineage section above.

Stages 7-10, 60 to ~ 500 cells (~ 7.5-16.5 hpl)

The next round of cell division was roughly synchronous in all cells in the embryo except in the AVPp and PVAa lineages (Fig. 5). Four cells, the daughters of AVPp and PVAa, delayed division, resulting in a 60 cell embryo at 6.5-8.5 hpl (stage 7, Fig. 5 and Fig. 7G). Three of the four cells with delayed cell division were the first to move to the center of the embryo, with either AVPpa or PVAap moving in first, followed by both AVPpp and PVAaa, at 7.5-8.5 hpl (stage 8, Fig. 7H; Movies S3 and S4). This was the first directed cell movement that was visible in the embryo. These three cells were followed by approximately 30-40 more cells that moved from the ventral surface to the interior of the embryo during the next three rounds of cell division, at 12-15 hpl (stage 9, Fig. 7I; Movie S3). As these movements occurred, the cell layer on the exterior of the embryo covered the ingression site by epiboly, forming a distinct epithelium, with no more ingressing cells apparent by 14-16.5 hpl (stage 10, Fig. 7J; Movie S3). Cells in this external epithelium were columnar, with the nuclei occupying the extreme apical end of each cell. At this point, the embryo was composed of approximately 500 cells. Cell divisions throughout the embryo occurred less frequently after this point.

Stage 11, elongation (~ 17 hpl)

Approximately 1 h after epiboly ended, the embryo began elongation (Fig. 8A; Movie S5). In this process, which occurred over approximately 3 h, the spherical embryo lengthened within the eggshell, resulting in a comma shape. At this point, anterior could be distinguished from posterior, with the developing anterior region forming the head of the comma, and the posterior region forming the tail of the comma. The elongated embryo consisted of an inner tube of cells, surrounded by an outer layer of cells, and based on their positions and following an endodermal marker (Gabriel and Goldstein, 2007), we speculate that these layers most likely contribute primarily endomesodermal and ectodermal derivatives, respectively.

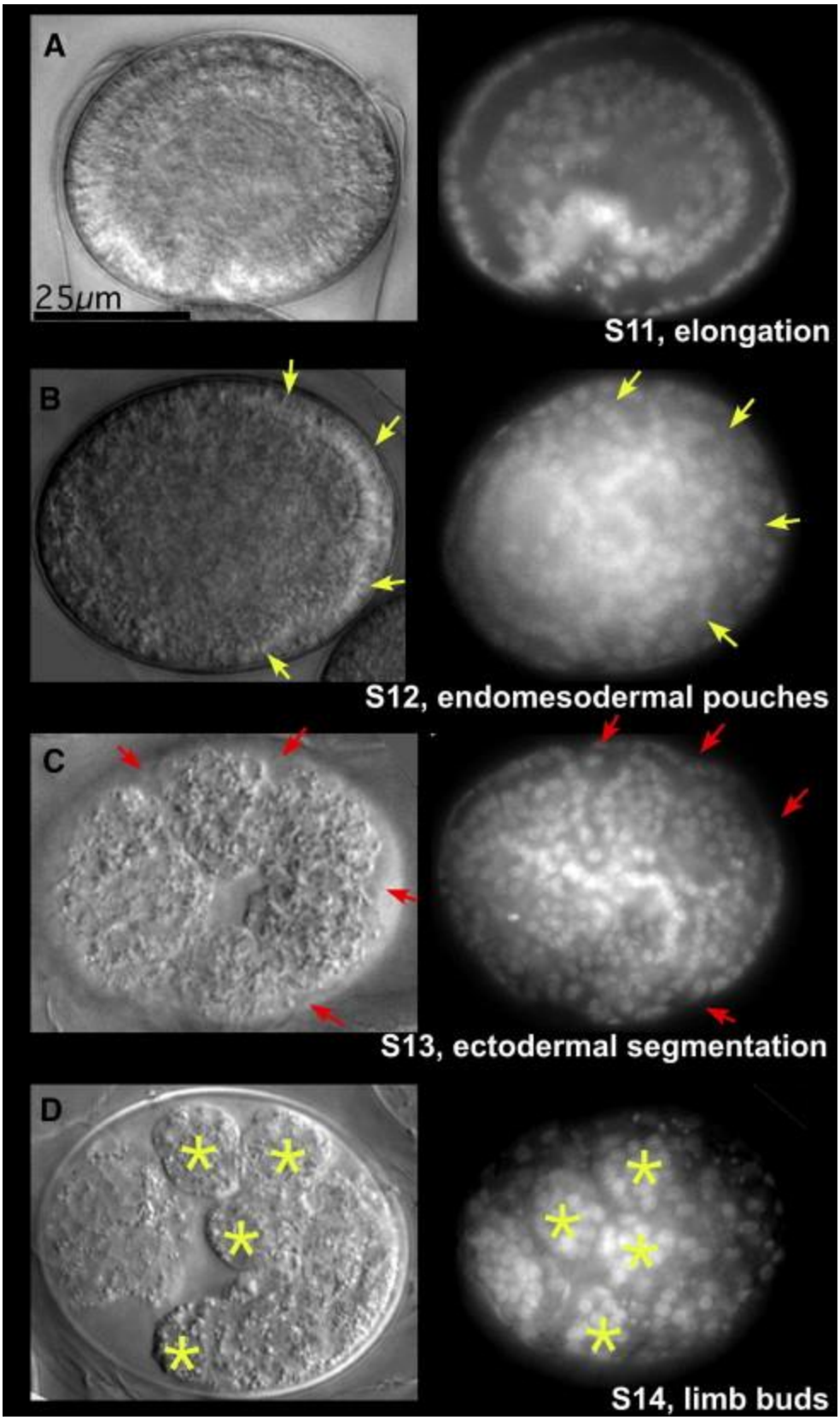

Fig. 8. Stages 11–14 of *H. dujardini* development. (A–D) *H. dujardini* embryos from elongation through limb bud formation (~ 17 to 26 hpl). All images are lateral views of embryos oriented with anterior to the left and ventral downwards. DIC images of live embryos

are on the left, and fixed embryos at the same developmental stage that have been stained with DAPI are on the right. Yellow arrows in panel B point to endomesodermal pouches. Red arrows in panel C point to the indentations in the ectoderm that mark segmental boundaries. Asterisks in panel D mark individual limb buds.

Figure options

Stages 12–13, appearance of segmental units (~ 21 hpl)

At the completion of elongation, the posterior half of the inner, presumably endomesodermal tube of cells constricted radially at four positions, producing four incompletely closed pouches of 20–30 cells per pouch at 21–23.5 hpl (stage 12, Fig. 8B; Movie S5). Pouch formation occurred in a posterior to anterior progression, with formation of the anterior-most pouch completed approximately 20 min after the posterior-most pouch formed. This was the earliest evidence of segmental differentiation that was visible by DIC microscopy, and it is accompanied by segmentally iterated expression of Engrailed and Pax3/7 homologs in the ectoderm (Gabriel and Goldstein, 2007). The endomesodermal pouches appeared to separate from the tube and form bilaterally paired structures.

Within 30 min to 2 h of pouch formation, the ectoderm began to constrict in the posterior of the embryo at positions in register with the boundaries of the endomesodermal pouches at 22–26 hpl (stage 13, Fig. 8C;Movie S6). These boundaries appeared to correspond to the sites of the segmental boundaries seen just before hatching.

Stage 14, limb bud formation (~ 26 hpl)

Limb buds began as lateral outgrowths of the ectoderm from either side of each segmental unit at ~ 26 hpl (Fig. 8D; Movie S6). We could not detect any cell division occurring in this region at this time. When the limb buds were fully extended (32–33 hpl), each limb bud had a radius of 3–4 cells (~ 10 μm) and a length of 5–6 cells (~ 18 μm). Except for the growth of claws, the limbs did not appear to differentiate further prior to hatching.

Prior to the start of limb bud formation, after the ectoderm became segmented, cells detached from the surface of the embryo into the vitelline space at numerous sites. This continued until the end of limb bud growth, by which time the embryo became enclosed in a cuticle that excluded the detached cells. Loose cells were seen in the vitelline space of embryos that were filmed, and in stage 14 embryos that were mounted without previous filming, suggesting they are not artifacts of filming.

Stage 15, pharynx and buccal apparatus (~ 28.5–38.5 hpl)

The pharynx and buccal apparatus that will ultimately comprise the feeding structures in *H. dujardini* were first visible as distinct structures at this stage (Fig. 9A). The buccal apparatus was first visible as a sphere of cells that pinched off from the anterior-most portion of the stomodaeum. The pharynx was visible as a sphere of cells immediately posterior to the buccal apparatus, also forming from the stomodaeum. Both pharynx and buccal apparatus consisted of 1–2 cell layers when they were first formed.

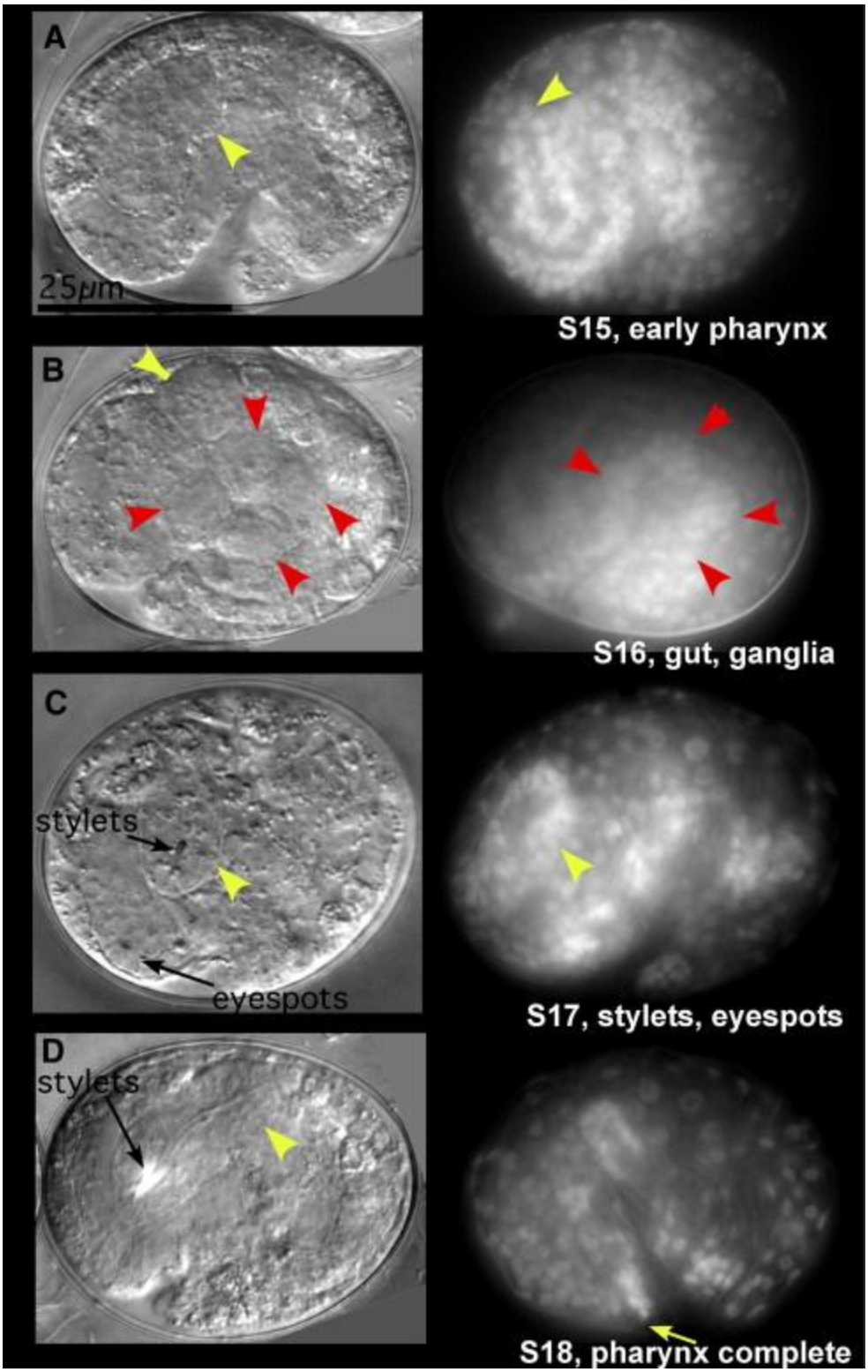

Fig. 9. Stages 15‑18 of *H. dujardini* development. (A‑D) *H. dujardini* embryos from ~ 28.5 to 65 hpl. All images are lateral views of embryos oriented with anterior to the left and ventral downwards. DIC images of live embryos are on the left, and fixed embryos at the same developmental stage that have been stained with DAPI are on the right. Yellow arrowheads point to the developing pharynx. The developing buccal apparatus is immediately anterior to the pharynx. Red arrowheads in panel B point to developing ganglia. Yellow arrow in panel D points to the mouth opening.

Figure options

Stage 16, ganglia and midgut (~ 38-50 hpl)

The ganglia were visible as four aggregations of cells along the ventral side, medial to and in register with the pairs of limb buds (Fig. 9B). The midgut could be seen as a distinct structure, dorsal to the limb buds. Endodermal identity of the midgut cells could be confirmed by the presence of birefringent granules (Gabriel and Goldstein, 2007).

Stage 17, muscle twitching, stylets, claws, and eyespots (~ 40-50 hpl)

Muscle contractions began ~ 15-25 h after limb buds had formed. Peristalsis of the midgut was the first visible contractile behavior. By approximately 5 h after peristalsis began, the embryo was rotating inside the eggshell. Claws also first appeared at this stage. Eyespots were visible as two small, black dots lateral to the developing pharynx (Fig. 9C; Movie S7). Stylets could first be distinguished in the developing buccal apparatus by birefringence.

Stage 18, pharynx and buccal apparatus morphologically distinct (~ 52-65 hpl)

The pharynx and buccal apparatus became distinct structures that consisted of 1-4 layers of cells and appeared to be bound by basal lamina (Fig. 9D). By this stage, the stylets had grown to almost the length of the buccal apparatus and were occasionally seen protruding from the mouth.

Stage 19, hatching

Embryos hatched 4 to 4.5 days after being laid. The embryo appeared to use its stylets to puncture its eggshell, after which the newly hatched tardigrade crawled out of the opening near the mouth, into the parental exuvia, and then out of the exuvia. The juveniles began walking and feeding after hatching (Movie S8).

Discussion

In this report, we have introduced the tardigrade *H. dujardini* as a new model system for studies on evolution of development. We have described characteristics that make *H. dujardini* a useful laboratory species, including ease of maintaining stocks and a short generation time. We have shown that *H. dujardini* has a compact genome, making it an attractive candidate for genome sequencing, as no tardigrade genome has yet been sequenced, and that the inferred rates of sequence evolution for this species are typical. To provide a standardized description of embryonic development for this species, we have generated a cell lineage and a staging series of 19 embryonic stages. Additionally, we have developed laboratory techniques to study this species including 4D videomicroscopy, fixation and DAPI staining protocols, and an embryo immunostaining protocol (Gabriel and Goldstein, 2007). Together, this information provides a platform for further studies using *H. dujardini* as a model for studying the evolution of development.

Developing methods to disrupt gene function will be an important step to making further use of *H. dujardini* as a model organism. Reverse genetic tools such as RNA interference and morpholinos are worth testing, but given the 13-14 day generation time of *H. dujardini* and the ease with which animals can be cultured and cryopreserved, forward genetic approaches may be feasible as well. It would be useful to be able to both maintain clonal organisms and cross-fertilize organisms as needed, but only parthenogenetic females have been recognized in our cultures to date. Males of *H. dujardini* have been described by others (Ramazzotti and Maucci, 1983) but do not appear to be present in our cultures. It may be possible to find specific conditions under which males can develop, although to our knowledge, there are no reports of facultative parthenogenesis in tardigrades. Alternatively, it may be possible to backcross males from other populations of *H. dujardini* to generate males in our stock.

We have recognized early indicators of the dorso-ventral axis in *H. dujardini* embryos. This has allowed us to align embryos between individuals and, as a result, recognize several stereotyped features in the early embryonic lineage. For example, we recognized unequal cell divisions as invariably unequal only once embryos could be considered from a consistent orientation, allowing cells to be identified reproducibly. Previous studies of development in another tardigrade species did not find reliable markers for orienting the early embryos (Hejnol and Schnabel, 2005). Hejnol and Schnabel called the cleavage pattern of *T. stephaniae* indeterminate. Could this be an artifact of a failure to recognize reliable early markers of the embryonic axes? This seems unlikely, as Hejnol and Schnabel (2005) could show that partial embryos produced by laser ablation could produce entire, small juvenile tardigrades, suggesting that cell fates are not determined early in this species. We suggest instead that *H. dujardini* has a more stereotyped pattern of early divisions than does *T. stephaniae*, and that cell fates may be determined earlier in *H. dujardini*. Performing similar laser ablations in *H. dujardini* will be useful to test this hypothesis. Variations in cell fate specification mechanisms between taxa have been seen previously in other phyla (Félix and Barrière, 2005).

Although *H. dujardini* and *T. stephaniae* are similar in many aspects, their embryos exhibit some interesting differences in modes of gastrulation and germ layer formation. During gastrulation in *H. dujardini*, cells appear to move to the interior of the embryo through a single opening, whereas cells of *T. stephaniae* also ingress through a separate, posterior opening and then move to the surface, filling the opening (Hejnol and Schnabel, 2005). The blastopore opening in *H. dujardini*, on the other hand, is closed by epiboly of the ectodermal cells. Another notable difference exists in the mode of formation of mesoderm in these two species. While in *H. dujardini* at least some of the mesodermal cells form from the endomesodermal pouches we have described, Hejnol and Schnabel (2005) described the formation of mesodermal somites in *T. stephaniae* embryos from precursors immediately under the ectoderm that were never associated with endodermal cells. The *H. dujardini* mode, thus, seems more similar to the formation of mesoderm by enterocoely as described by von Erlanger (1895) and Marcus (1929). This is an interesting difference, and one that is unlikely to be an artifact, since descriptions of these processes in both species were made by detailed analysis of 4D DIC films. It will be of interest to examine whether this difference is accompanied by earlier mesodermal cell fate determination in *T. stephaniae* embryos than in *H. dujardini* by examining markers of germ-layer differentiation in these species.

The cell lineage we have produced extends about as far as ascidian, leech, and almost any metazoan cell lineage outside of the nematodes in terms of number of rounds of division and number of cells (Sulston et al., 1983, Nishida, 1997, Weisblat et al., 1999 and Houthoofd et al., 2003), but it lacks an important feature of these other lineages–the identification of the fate of each cell. Previous authors have assigned cell fates in tardigrades based on embryonic cell positions before tissues could be unambiguously identified (Marcus, 1929, for example). To avoid guesswork, clear markers of cell fates in lineage-traced embryos are needed. We have found, for example, that an enrichment of alkaline phosphatase activity and birefringent granules are early markers of endodermal cells (Gabriel and Goldstein, 2007). However, a gap remains between the furthest we have traced lineages to date (the 8th round of division in most but not all lineages) and when these markers appear (W.N.G., S.K.P. and B.G., unpublished). Cleavage-arrest (Whittaker, 1973) or injection of cells with lineage tracers (Weisblat et al., 1980) may be useful ways to bridge this gap in the future.

We have found that *H. dujardini* has a compact genome. Given that genome size is among the criteria considered important in the future choice of both complete sequencing targets (Gregory, 2005) and developmental models (Jenner and Wills, 2007 and Milinkovitch and Tzika, 2007), *H. dujardini* may be well poised to make contributions to an improved understanding of tardigrade biology and cryptobiosis in particular and of genomic and developmental evolution more generally. Tardigrades may additionally serve as a useful outgroup to large groups of existing evolutionary developmental models among the arthropods and the nematodes, providing another source to help identify the ancestral states of evolutionary changes that have occurred within the arthropods or within the nematodes.

Study organisms chosen in evolutionary developmental biology are often satellite organisms of a specific, well-studied developmental model. The well-studied model can provide a rich source of information about which genes control morphology. This has been a very successful starting point for identifying the evolutionary changes to developmental mechanisms that have driven morphological evolution (for reviews, see Davis and Patel, 2002 and Carroll, 2005). Which genes control morphology can change through evolution, so this strategy is generally more difficult to implement as evolutionary distance from a model increases. By choosing an organism that is a satellite of two well-studied models, it is our hope that in the long run, the genes that control morphology through evolution can be identified more reliably over a large evolutionary distance and that this can help make unique contributions to understanding morphological evolution.

Note added in proof

The NIH National Human Genome Research Institute has recently approved sequencing of the *H. dujardini*genome by the Broad Institute's Genome Biology Program.

Acknowledgments

This work was supported by a Pew Scholars Award and National Science Foundation grant IBN-0235658 (to BG), and a Natural Sciences and Engineering Research Council of Canada Discovery Grant (to TRG). The authors thank R. Bertolani, I. Dworkin, G. Freeman, D. Nelson, J. Reinhardt, D. Weisblat, and members of the Goldstein lab for comments on the manuscript; R. Bertolani for identifying the species of tardigrade used; D. Ammermann for discussions; D. Nelson for advice on SEM and on rearing tardigrades; M. Blaxter for leading BG to RM and for making EST and GSS sequence data available on Genbank before publication; C. Beasley for an English translation

of Ramazzotti and Maucci (1983); A. Ardila Garcia for assistance with the flow cytometry analysis; and S. Brenner for discussing the details of his pre-*C. elegans* foray into tardigrades.

Appendix A. Supplementary data

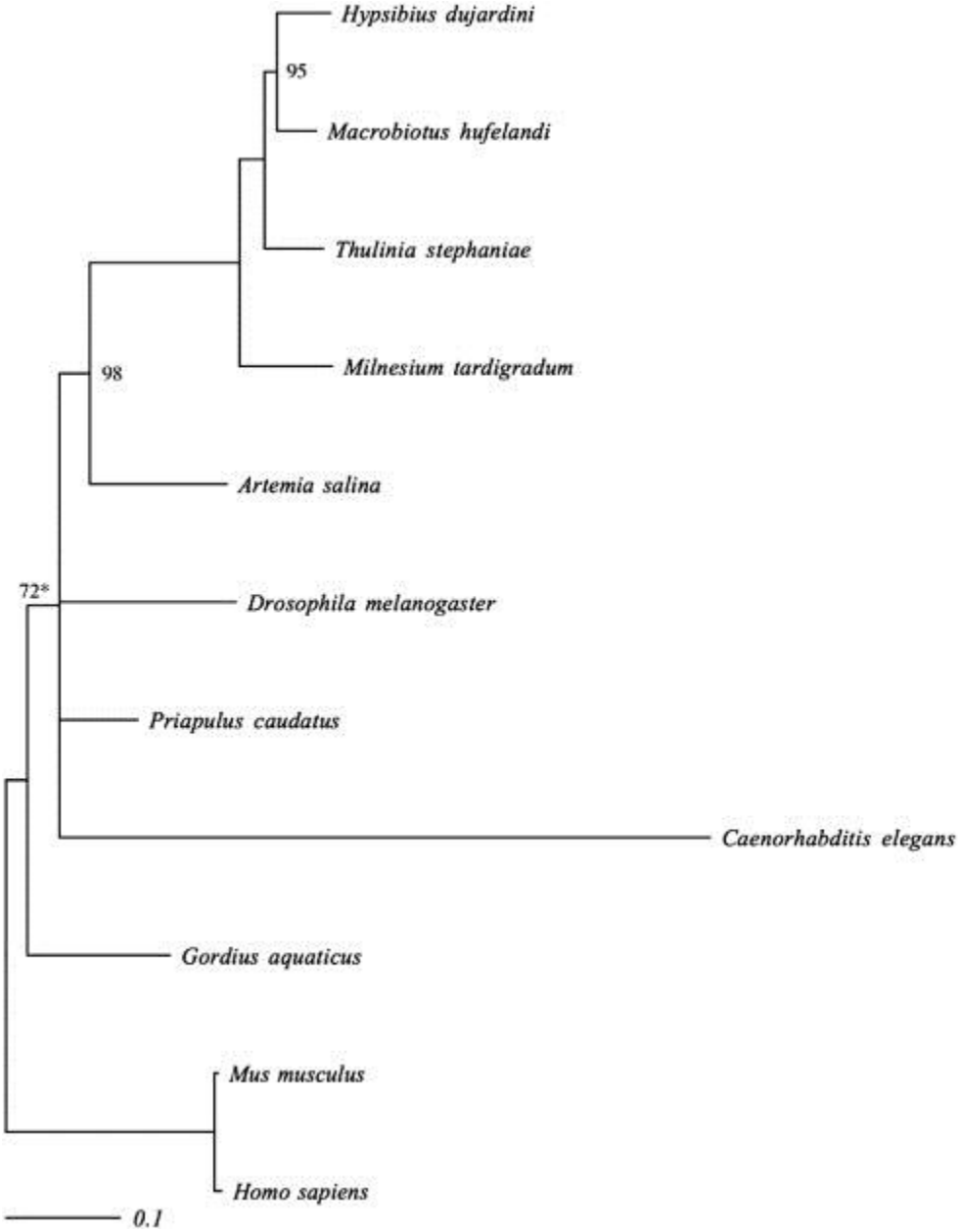

Fig. S1. Concatenated gene tree (upper left) and five representative gene trees from among 21 genes that were phylogenetically analyzed. Trees were built using a Bayesian approach (see Materials and methods). Any node with credibility score below 100% is annotated. Nodes below 80% credibility are considered unresolved. Branch lengths are noted on the concatenated tree as mean numbers of amino acid substitutions per site, and scale bars for mean numbers of amino acid substitutions per site are shown for the five representative gene trees. As concatenated sequence trees can be problematic (Edwards et al., 2007 and Kubatko and Degnan, 2007), we used the concatenated sequence tree only for illustration purposes and not for the analysis of rates of amino acid evolution.
Figure options

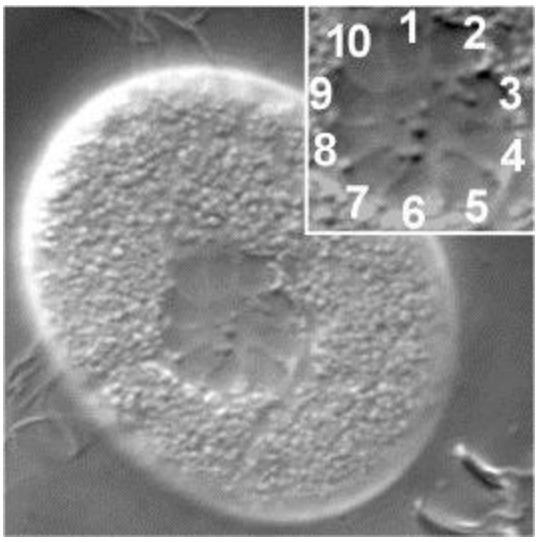

Fig. S2. Embryo in meiosis. Inset shows individual chromosomes counted (2n = 10).
Figure options
Movie S1. Two embryos from the 8 cell stage (stage 4) through the initiation of segmentation (stage 13).
Help with MOV files
Options
Movie S2. Two embryos from after the initiation of segmentation (stage 13) through hatching (stage 19).
Help with MOV files
Options
Movie S3. Embryo from stages 7–10. Ingression begins at the start of the film and continues as epiboly begins. Black arrowhead points to the site at which ingression begins.
Help with MOV files
Options
Movie S4. Embryo at stage 7, viewed from ventral surface. Asterisks mark the four cells that can ingress; three of these cells ingress. This is the same embryo shown in Fig. 6B. Time elapsed is in h:min:s.
Help with MOV files
Options
Movie S5. Two embryos from stages 10–12. Embryos have formed an epithelium at the beginning of the film and subsequently undergo elongation. Endomesodermal pouches are evident in the embryo on the left (arrowheads at end of film). Anterior (A) and posterior (P) are labeled in the last frames of the film. Arrows point to the space between the future head and tail of the embryos.
Help with MOV files
Options
Movie S6. Two embryos from stages 13–14. Ectodermal furrows are evident in embryos at the beginning of the film (arrowheads), and limb buds form subsequently (asterisks). Detached cells are visible inside the eggshell throughout this film.
Help with MOV files
Options
Movie S7. Two embryos beginning muscle twitching. The pharynx (arrowheads) and buccal structure (arrows) are visible in both embryos.
Help with MOV files
Options
Movie S8. Three hatched juveniles walking and feeding on algae. Polarized light view, with birefringent granules in endodermal cells and birefringent stylets visible. Time elapsed is in h:min:s.
Help with MOV files
Options

References

Aguinaldo et al., 1997
A.M. Aguinaldo, J.M. Turbeville, L.S. Linford, M.C. Rivera, J.R. Garey, R.A. Raff, J.A. Lake
Evidence for a clade of nematodes, arthropods and other moulting animals
Nature, 387 (1997), pp. 489–493
View Record in Scopus

Full Text via CrossRef
| Cited By in Scopus (955)

Altiero and Rebecchi, 2001
T. Altiero, L. Rebecchi
Rearing tardigrades: results and problems
Zool. Anz., 240 (2001), pp. 217–221
Article
|
PDF (86 K)
|
View Record in Scopus
|
Full Text via CrossRef
| Cited By in Scopus (17)

Ammermann, 1967
D. Ammermann
Die Cytologie der Parthenogenese bei dem Tardigraden *Hypsibius dujardini*
Chromosoma, 23 (1967), pp. 203–213
View Record in Scopus
|
Full Text via CrossRef
| Cited By in Scopus (11)

Ammermann and Bosse, 1968
D. Ammermann, C. Bosse
Wasserbären
Mikrokosmos, 57 (1968), pp. 24–27

Anderson, 1973
D. Anderson
Embryology and Phylogeny in Annelids and Arthropods
Pergammon Press, Oxford (1973)

Bertolani et al., 1994
R. Bertolani, S. Garagna, G. Manicardi, L. Rebecchi, C. Redi
New data on the nuclear DNA content in some species of tardigrades
Anim. Biol. (1994), pp. 103–109

Bertolani et al., 2004
R. Bertolani, R. Guidetti, I. Jönsson, T. Altiero, D. Boschini, L. Rebecchi
Experiences with dormancy in tardigrades
J. Limnol., 63 (2004), pp. 16–25
View Record in Scopus
| Cited By in Scopus (26)

Bishop and Friday, 1987
M. Bishop, A. Friday

Tetrapod relationships: the molecular evidence
C. Patterson (Ed.), Molecules and Morphology in Evolution: Conflict or Compromise?, Cambridge University Press, Cambridge (1987), pp. 123–139

Brenner, 2001
S. Brenner
My Life in Science
Biomed Central Ltd., London (2001)

Carroll, 2005
S.B. Carroll
Evolution at two levels: on genes and form
PLoS Biol., 3 (2005), p. e245
View Record in Scopus
|
Full Text via CrossRef
| Cited By in Scopus (109)

Copley et al., 2004
R.R. Copley, P. Aloy, R.B. Russell, M.J. Telford, J.P. Huelsenbeck, F. Ronquist
Systematic searches for molecular synapomorphies in model metazoan genomes give some support for Ecdysozoa after accounting for the idiosyncrasies of *Caenorhabditis elegans*
Evol. Dev., 6 (2004), pp. 164–169

Davis and Patel, 2002
G.K. Davis, N.H. Patel
Short, long, and beyond: molecular and embryological approaches to insect segmentation
Annu. Rev. Entomol., 47 (2002), pp. 669–699

Dayhoff et al., 1978
M. Dayhoff, R. Schwartz, B. Orcutt
A model for evolutionary change in proteins
M. Dayhoff (Ed.), Atlas of Protein Sequence and Structure, Vol. 5 (1978), pp. 345–352

De Rosa et al., 1999
R. de Rosa, J.K. Grenier, T. Andreeva, C.E. Cook, A. Adoutte, M. Akam, S.B. Carroll, G. Balavoine
Hox genes in brachiopods and priapulids and protostome evolution
Nature, 399 (1999), pp. 772–776

De Salle et al., 2005
R. De Salle, T.R. Gregory, J.S. Johnston
Preparation of samples for comparative studies of arthropod chromosomes: visualization, in situ hybridization, and genome size estimation
Methods Enzymol., 395 (2005), pp. 460–488

Deppe et al., 1978

U. Deppe, E. Schierenberg, T. Cole, C. Krieg, D. Schmitt, B. Yoder, G. von Ehrenstein
Cell lineages of the embryo of the nematode *Caenorhabditis elegans*
Proc. Natl. Acad. Sci. U. S. A., 75 (1978), pp. 376-380

Dopazo and Dopazo, 2005
H. Dopazo, J. Dopazo
Genome-scale evidence of the nematode-arthropod clade
Genome Biol., 6 (2005), p. R41

Doyère, 1840
L. Doyère
Memoire sur les tardigrades
Ann. Sci. Zool. Ser. 2, 14 (1840), pp. 269-361

Edwards et al., 2007
S.V. Edwards, L. Liu, D.K. Pearl
High-resolution species trees without concatenation
Proc. Natl. Acad. Sci. U. S. A., 104 (2007), pp. 5936-5941

Eibye-Jacobsen, 1997
J. Eibye-Jacobsen
New observations on the embryology of the Tardigrada
Zool. Anz., 235 (1997), pp. 201-216

Eriksson et al., 2005
B.J. Eriksson, E.T. Larson, P. Thornqzist, N.N. Tait, G.E. Budd
Expression of engrailed in the developing brain and appendages of the onychophoran*Euperipatoides kangaransis* (Reid)
J. Exp. Zool., 304B (2005), pp. 1-9

Félix and Barrière, 2005
M.A. Félix, A. Barrière
Evolvability of cell specification mechanisms
J. Exp. Zoolog. B Mol. Dev. Evol., 304 (2005), pp. 536-547
View Record in Scopus
|
Full Text via CrossRef
| Cited By in Scopus (9)

Gabriel and Goldstein, 2007
W.N. Gabriel, B. Goldstein
Segmental expression of Pax3/7 and Engrailed homologs in tardigrade development
Dev. Genes Evol., 217 (2007), pp. 421-433
View Record in Scopus
|
Full Text via CrossRef
| Cited By in Scopus (16)

Garey, 2001
J.R. Garey
Ecdysozoa: the relationship between the Cyclomeuralia and Panarthropoda
Zool. Anz., 240 (2001), pp. 321–330
Article
|
PDF (165 K)
|
View Record in Scopus
|
Full Text via CrossRef
| Cited By in Scopus (38)

Garey et al., 1999
J.R. Garey, D.R. Nelson, L.Y. Mackey, J. Li
Tardigrade phylogeny: congruency of morphological and molecular evidence
Zool. Anz., 238 (1999), pp. 205–210

Gerberding et al., 2002
M. Gerberding, W.E. Browne, N.H. Patel
Cell lineage analysis of the amphipod crustacean *Parhyale hawaiensis* reveals an early restriction of cell fates
Development, 129 (2002), pp. 5789–5801
View Record in Scopus
|
Full Text via CrossRef
| Cited By in Scopus (51)

Giribet and Ribera, 1998
G. Giribet, C. Ribera
The position of arthropods in the animal kingdom: a search for a reliable outgroup for internal arthropod phylogeny
Mol. Phylogenet. Evol., 9 (1998), pp. 481–488
Article
|
PDF (125 K)
|
View Record in Scopus
| Cited By in Scopus (74)

Goldstein, 2001
B. Goldstein
On the evolution of early development in the Nematoda
Philos. Trans. R. Soc. Lond., Ser. B Biol. Sci., 356 (2001), pp. 1521–1531
View Record in Scopus
|
Full Text via CrossRef
| Cited By in Scopus (17)

Greenwald and Rubin, 1992
I. Greenwald, G.M. Rubin

Making a difference: the role of cell-cell interactions in establishing separate identities for equivalent cells
Cell, 68 (1992), pp. 271-281
Article
|
PDF (1399 K)
|
View Record in Scopus
| Cited By in Scopus (198)

Gregory, 2001
T.R. Gregory
Coincidence, coevolution, or causation? DNA content, cell size, and the C-value enigma
Biol. Rev. Camb. Philos. Soc., 76 (2001), pp. 65-101

Gregory, 2005
T.R. Gregory
Synergy between sequence and size in large-scale genomics
Nat. Rev., Genet., 6 (2005), pp. 699-708

Gregory, 2007
T.R. Gregory
Eukaryotic genome size databases
Nucleic Acids Res., 35 (2007), pp. D332-D338

Grenier and Carroll, 2000
J.K. Grenier, S.B. Carroll
Functional evolution of the Ultrabithorax protein
Proc. Natl. Acad. Sci. U. S. A., 97 (2000), pp. 704-709

Guidetti and Bertolani, 2005
R. Guidetti, R. Bertolani
Tardigrade taxonomy: an updated check list of the taxa and a list of characters for their identification
Zootaxa, 845 (2005), pp. 1-46

Guil and Cabrero-Sañudo, 2007
N. Guil, F.J. Cabrero-Sañudo
Analysis of the species description process for a little known invertebrate group: the limnoterrestrial tardigrades (Bilateria, Tardigrada)
Biodivers. Conserv., 16 (2007), pp. 1063-1086

Hardie et al., 2002
D.C. Hardie, T.R. Gregory, P.D. Hebert
From pixels to picograms: a beginners' guide to genome quantification by Feulgen image analysis densitometry
J. Histochem. Cytochem., 50 (2002), pp. 735-749

Hejnol and Schnabel, 2005
A. Hejnol, R. Schnabel
The eutardigrade *Thulinia stephaniae* has an indeterminate development and the potential to regulate early blastomere ablations
Development, 132 (2005), pp. 1349–1361

Hertzler and Clark, 1992
P.L. Hertzler, W.H. Clark Jr.
Cleavage and gastrulation in the shrimp *Sicyonia ingentis*: invagination is accompanied by oriented cell division
Development, 116 (1992), pp. 127–140
View Record in Scopus
| Cited By in Scopus (47)

Houthoofd et al., 2003
W. Houthoofd, K. Jacobsen, C. Mertens, S. Vangestel, A. Coomans, G. Borgonie
Embryonic cell lineage of the marine nematode *Pellioditis marina*
Dev. Biol., 258 (2003), pp. 57–69
Article
|
PDF (444 K)
|
View Record in Scopus
| Cited By in Scopus (27)

Huelsenbeck and Ronquist, 2001
J.P. Huelsenbeck, F. Ronquist
MRBAYES: Bayesian inference of phylogenetic trees
Bioinformatics, 17 (2001), pp. 754–755
View Record in Scopus
|
Full Text via CrossRef
| Cited By in Scopus (72)

Hyman, 1951
L.H. Hyman
The Invertebrates. Volume 3, Acanthocephala, Aschelminthes, and Entoprocta
McGraw-Hill Book Company, Inc., New York and London (1951)

Jenner and Wills, 2007
R.A. Jenner, M.A. Wills
The choice of model organisms in evo-devo
Nat. Rev., Genet., 8 (2007), pp. 311–314
Full Text via CrossRef

Jones et al., 1992
D.T. Jones, W.R. Taylor, J.M. Thornton
The rapid generation of mutation data matrices from protein sequences
Comput. Appl. Biosci., 8 (1992), pp. 275–282
View Record in Scopus
| Cited By in Scopus (2109)

Kinchin, 1994
I. Kinchin
The Biology of Tardigrades
Portland Press, London (1994)

Kubatko and Degnan, 2007
L.S. Kubatko, J.H. Degnan
Inconsistency of phylogenetic estimates from concatenated data under coalescence
Syst. Biol., 56 (2007), pp. 17–24
View Record in Scopus
|
Full Text via CrossRef
| Cited By in Scopus (223)

Malakhov, 1994
V.V. Malakhov
Nematodes: Structure, development, classification, and phylogeny
Smithsonian Institution Press, Washington, DC (1994)

Marcus, 1929
E. Marcus
Zur embryologie der tardigraden
Zool. Jahrb., 50 (1929), pp. 333–384

Milinkovitch and Tzika, 2007
M.C. Milinkovitch, A. Tzika
Escaping the mouse trap: the selection of new Evo-Devo model species
J. Exp. Zoolog. B Mol. Dev. Evol., 308 (2007), pp. 337–346
View Record in Scopus
|
Full Text via CrossRef
| Cited By in Scopus (16)

Müller et al., 1995
K. Müller, D. Walossek, A. Zakharov
'Orsten' type phosphatised soft-integument preservation and a new record from the middle Cambrian Kuonamka Formation in Siberia
Neues Jahrb. Geol. Paläontol. Abh., 197 (1995), pp. 101–118

Mushegian et al., 1998
A.R. Mushegian, J.R. Garey, J. Martin, L.X. Liu
Large-scale taxonomic profiling of eukaryotic model organisms: a comparison of orthologous proteins encoded by the human, fly, nematode, and yeast genomes
Genome Res., 8 (1998), pp. 590–598

Nichols et al., 2006
B. Nichols, D.R. Nelson, J.R. Garey

A family level analysis of tardigrade phylogeny
Hydrobiologia, 558 (2006), pp. 53‐60

Nishida, 1997
H. Nishida
Cell lineage and timing of fate restriction, determination and gene expression in ascidian embryos
Semin. Cell Dev. Biol., 8 (1997), pp. 359‐365

Page, 1996
R.D. Page
TreeView: an application to display phylogenetic trees on personal computers
Comput. Appl. Biosci., 12 (1996), pp. 357‐358

Panganiban et al., 1997
G. Panganiban, S.M. Irvine, C. Lowe, H. Roehl, L.S. Corley, B. Sherbon, J.K. Grenier, J.F. Fallon, J. Kimble, M. Walker, G.A. Wray, B.J. Swalla, M.Q. Martindale, S.B. Carroll
The origin and evolution of animal appendages
Proc. Natl. Acad. Sci. U. S. A., 94 (1997), pp. 5162‐5166

Peterson and Eernisse, 2001
K.J. Peterson, D.J. Eernisse
Animal phylogeny and the ancestry of bilaterians: inferences from morphology and 18S rDNA gene sequences
Evol. Dev., 3 (2001), pp. 170‐205

Ramazzotti and Maucci, 1983
G. Ramazzotti, W. Maucci
Il Phylum Tardigrada
(2nd ed.)Memorie dell'Istituto italiano Idrobiologia dott, Marco de Marchi (1983) vol. 41

Schmidt, 1971
Schmidt
Hypsibius dujardini (Tardigrada)–Organisation und Fortpflanzung
Film, IWF (Göttingen) (1971)

Simpson, 1997
P. Simpson
Notch signalling in development: on equivalence groups and asymmetric developmental potential
Curr. Opin. Genet. Dev., 7 (1997), pp. 537‐542
Article
|
PDF (459 K)
|
View Record in Scopus
| Cited By in Scopus (106)

Stiernagle, 2006

Stiernagle, T., 2006. Maintenance of *C. elegans* (February 11, 2006), WormBook, ed. The C. elegans Research Community, WormBook, 10.1895/wormbook.1.101.1, http://www.wormbook.org.

Sulston et al., 1983
J.E. Sulston, E. Schierenberg, J.G. White, J.N. Thomson
The embryonic cell lineage of the nematode *Caenorhabditis elegans*
Dev. Biol., 100 (1983), pp. 64-119
Article
|
PDF (12813 K)
|
View Record in Scopus
| Cited By in Scopus (1441)

Thomas et al., 1996
C. Thomas, P. DeVries, J. Hardin, J. White
Four-dimensional imaging: computer visualization of 3D movements in living specimens
Science, 273 (1996), pp. 603-607
View Record in Scopus
|
Full Text via CrossRef
| Cited By in Scopus (83)

Thompson et al., 1994
J.D. Thompson, D.G. Higgins, T.J. Gibson
CLUSTAL W: improving the sensitivity of progressive multiple sequence alignment through sequence weighting, position-specific gap penalties and weight matrix choice
Nucleic Acids Res., 22 (1994), pp. 4673-4680
View Record in Scopus
| Cited By in Scopus (38834)

Von Erlanger, 1895
R. von Erlanger
Beiträge zur Morphologie der Tardigraden: I. Zur Embryologie eines Tardigraden: Macrobiotus macronyx Dujardin
Morph. Jb., 22 (1895), pp. 491-513

Von Wenck, 1914
W. von Wenck
Entwicklungsgeschichtliche Untersuchungen an Tardigraden (*Macrobiotus lacustris*Duj.)
Zool. Jb. Anat., 37 (1914), pp. 465-514

Weisblat et al., 1980
D.A. Weisblat, S.L. Zackson, S.S. Blair, J.D. Young
Cell lineage analysis by intracellular injection of fluorescent tracers
Science, 209 (1980), pp. 1538-1541
View Record in Scopus
| Cited By in Scopus (18)

Weisblat et al., 1999
D.A. Weisblat, F.Z. Huang, D.E. Isaksen, N.J. Liu, P. Chang

The other side of the embryo: an appreciation of the non-D quadrants in leech embryos
Curr. Top. Dev. Biol., 46 (1999), pp. 105–132
Article
|
PDF (2047 K)
|
View Record in Scopus
| Cited By in Scopus (4)

Whittaker, 1973
J.R. Whittaker
Segregation during ascidian embryogenesis of egg cytoplasmic information for tissue-specific enzyme development
Proc. Natl. Acad. Sci. U. S. A., 70 (1973), pp. 2096–2100
View Record in Scopus
|
Full Text via CrossRef
| Cited By in Scopus (77)

Wright, 1989
J. Wright
Desiccation tolerance and water-retentive mechanisms in tardigrades
J. Exp. Biol., 142 (1989), pp. 267–292

Wright, 2001
J. Wright
Cryptobiosis 300 years on from van Leuwenhoek: what have we learned about tardigrades?
Zool. Anz., 240 (2001), pp. 563–582
Article
|
PDF (284 K)
|
View Record in Scopus
|
Full Text via CrossRef
| Cited By in Scopus (65)

Corresponding author. Fax: +1 919 962 1625.